

# Stress Relaxation Measurements of Meta-dynamic and Static Recrystallization of Alloy 80A

S. Kleber<sup>1</sup> and C. Sommitsch<sup>1</sup>

<sup>1</sup> Böhler Edelstahl GmbH, P.O.BOX 96, A-8605 Kapfenberg, Austria

**Keywords:** metadynamic recrystallization, static recrystallization, stress relaxation.

**Abstract.** The stress relaxation method has been applied to the nickel-based alloy 80A to predict meta-dynamic (MDRX) and static recrystallization (SRX) kinetics. Compression tests were performed on a Gleeble 3800 system at different temperatures (950-1200°C). The strain rate was varied in the case of MDRX and the pre-strain in the case of SRX. To investigate MDRX, the pre-strain was set to twice the peak strain in order to reach steady state before holding. To focus on the interaction of MDRX and SRX, the pre-strain was set to the peak strain, where dynamic recrystallization (DRX) starts but does not yet reach steady state. Avrami type equations for the prediction of both the MDRX and SRX were adapted to feed a semi-empirical grain structure model.

## Introduction

During hot forming of nickel-based alloys DRX and MDRX have been shown to be the major softening mechanisms due to the low stacking fault energy of these types of alloys. However, recovery tends to become more important if the number of potential nuclei decreases [1]. The latter occurs in very coarse structured materials, e.g. in remelted structures of large ingots. Hence the primary deformation step in such a material should be done with great caution, having in mind that the deformation ability depends on temperature, deformation rate and initial grain size.

In the case of pre-deformed and homogeneous structures, semi-empirical equations can be used to describe the recrystallization kinetics [2]. If there is precipitation of small particles during recrystallization, the interaction will alter the kinetics fundamentally. With these simple models, only a splitting of the model parameters in several temperature regimes can be done. To verify a model, several techniques are well known, e.g. the stress relaxation method [3-4] and the double hit compression test [5-7]. The latter has the major disadvantage of needing much more experiments for the description of the recrystallization process. A second problem occurs when conducting tests at high deformation rates, where isothermal conditions can not be produced. In this case, the two stress-strain curves represent materials at different temperatures and thus can not be compared. For Gleeble compression tests with nickel-based alloys the critical deformation rate was found to be about  $1\text{s}^{-1}$ .

SRX is defined by the formation of nuclei after the deformation, MDRX shows the ongoing growth of dynamically recrystallized grains after straining. There are critical strains for the onset of SRX and DRX, both dependent on the temperature and the strain rate. Strictly, models for MDRX are only valid if the steady state of DRX (steady state strain) has been reached. If the pre-strain is between these two limits, the nucleation processes of SRX and the growth of dynamically recrystallized grains will interact during the interpass time and simple semi-empirical laws can not be used. Hence a part of this work will investigate the interaction of SRX and MDRX.

## Experiments

The stress relaxation method as an alternative to the double hit test has often been applied to measure the softening kinetics of austenite in steels [3]. For the investigation of both MDRX and

SRX, the experimental temperature, strain and strain rate ranges essentially depend on the material and the industrial process of interest, e.g. rolling or forging. For rod rolling or strip mills typically strain rates of more than  $100\text{s}^{-1}$  occur. Modern servo-hydraulic systems like the Gleeble system ensure those high strain rates for compression tests. In the case of the stress relaxation technique, the crucial point for these experiments at high strain rates appeared to be the instantaneous stopping and constant holding for longer time periods of the action cylinder after the straining sequence.

A large sized servo-valve controls the oil flow during straining, whereas a very accurate small sized valve guarantees the exact positioning of the cylinder during stress relaxation using minimal flow rates. A second important issue is the heating system of the simulation aggregate. There are both furnaces and inductive or conductive systems to heat the specimen and enable flexible time-temperature courses.

In this work, cylindrical compression tests were conducted with a Gleeble 3800<sup>TM</sup> system. The action cylinder is controlled by a staged servo-valve and the specimens are heated conductively by a filament transformer, which is governed by a thyristor on the primary side. Similar to the experimental setup of Karjalainen [3], both a graphite foil and foil made of tantalum or molybdenum are put between the compression specimen and the tungsten carbide overlay. The specific geometry and the character of the tools determine the temperature distribution within the specimen and the rate of heat release and heat production, respectively. Above a strain rate of about  $1\text{s}^{-1}$  and for nickel based alloys, the Gleeble system changes from isothermal to adiabatic behaviour. In general, nickel based alloys have a higher electrical resistance and a lower heat conductivity than austenitic steels. Thus temperature gradients decay relatively slowly due to the low local heat dissipation. As a matter of fact, thermo elements that are welded to the sample surface react relatively slowly to a temperature rise in the center of the specimen. Fig. 1 shows the measured temperature evolution both at the surface and in the center of the specimen with time during straining.

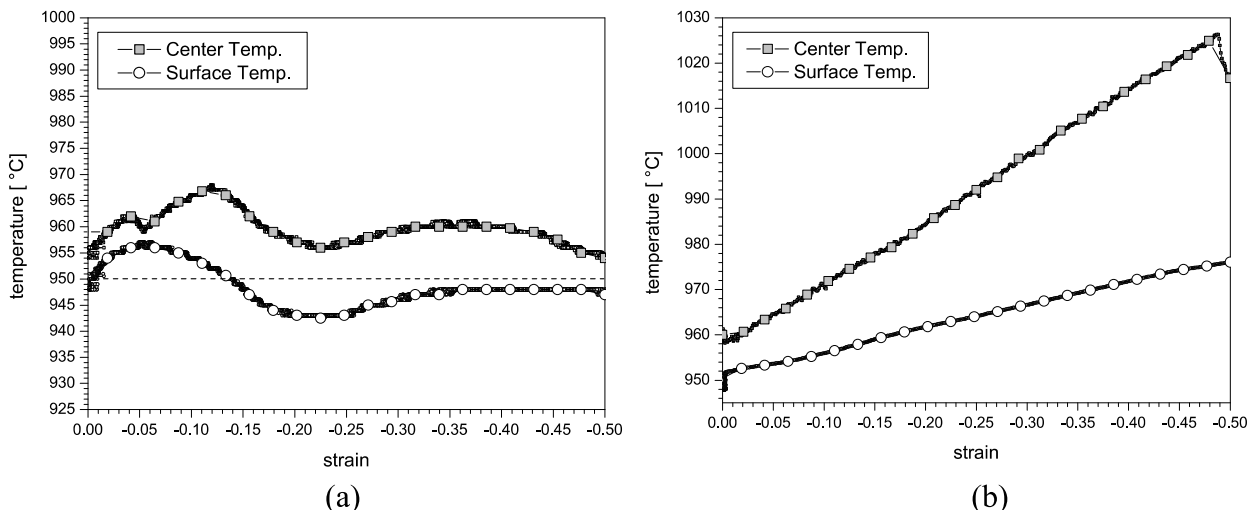


Fig. 1: Measured temperature evolution in the center and on the surface of the specimen for a target temperature of  $950^{\circ}\text{C}$  and for strain rates of  $0.1\text{s}^{-1}$  (a) and  $10\text{s}^{-1}$  (b).

In the case of adiabatic heating (strain rate of  $10\text{s}^{-1}$ ) the heating control experiences variations from the set point as a function of the strain and the initial temperature. The diameter to height ratio of the sample also changes during deformation and thus influences the thermal control. Unfavourably, the thermal control board usually reacts on these influences during stress relaxation and recrystallization, respectively. Hence, the numerical analysis can be complicated. This behaviour of the controlling system can be accounted for only in choosing the right PID settings to get a sound experimental program. The dynamic of the thermal control can not be increased arbitrarily because

of the fixed heating frequency of 50Hz. On the other hand, the reaction behaviour of the thermal system can be altered by a temporary variation of the power angle, which is in proportion to the energy release of the transformer. The power angle together with the stress relaxation and the temperature development is depicted in Fig. 2.

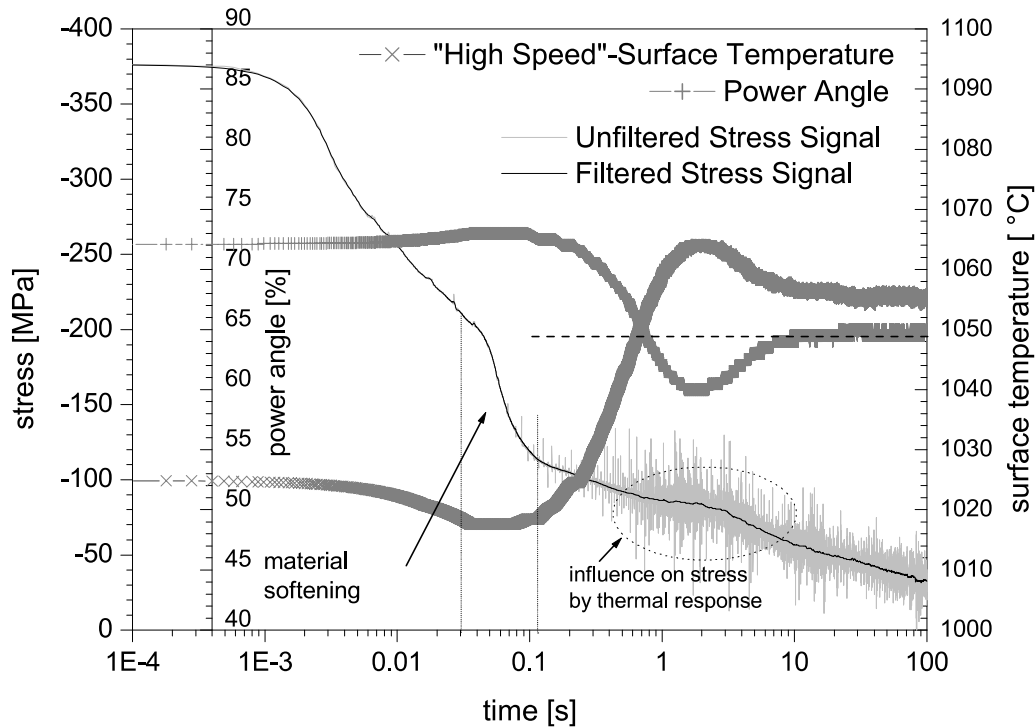


Fig. 2: Measured signals of a stress relaxation test with the initial surface temperature of 1050°C of the specimen at a logarithmic strain of 0.3 and a strain rate of  $10\text{s}^{-1}$ . “High Speed” measurement of the surface temperature is based on a specific measurement frequency of 10kHz.

**Experimental program for the investigation of meta-dynamic recrystallization.** Samples of Böhler L306 VMR (alloy 80A) were cut from hot rolled pieces, thus ensuring a completely recrystallized, fine-grained and homogeneous microstructure. Solution heat treatment was done at 1200°C for 120 seconds. The short annealing time was chosen to avoid grain growth. This lead to an initial grain size of 120 $\mu\text{m}$ . The specimens remained at 1200°C or were cooled down to the test temperatures of 1120, 1050 and 950°C by  $1\text{Ks}^{-1}$  and were compressed at a constant strain rate to strains  $\varepsilon = 2 \times \varepsilon_{\text{peak}}$  to ensure MDRX behaviour. The peak-strains  $\varepsilon_{\text{peak}}$  were estimated from flow curves which were recorded in a previous investigation by the identical test conditions [8]. The applied strain values can be taken from Table 1, which gives an overview of this test program.

**Experimental program for the investigation of static recrystallization.** The compression samples were again heat treated as described before, compressed at a constant strain rate to strains  $\varepsilon = 0.3, 0.5, 0.7$  and  $0.9 \times \varepsilon_{\text{peak}}$  to ensure SRX behaviour at the temperatures of 1050 and 1120°C. The strain rate variation was limited to  $\dot{\varepsilon} = 0.01, 0.1$  and  $10\text{s}^{-1}$  because a weak influence was supposed. Additional double hit tests were performed with  $\varepsilon = 0.1, 0.3, 0.5, 0.7, 0.9, 1.0, 1.3, 1.5, 1.7$  and finally  $2.0 \times \varepsilon_{\text{peak}}$  with a constant delay time of 2s to submit the exploitation of the relaxation test results. For the investigation of the interaction between SRX and MDRX further test with  $\varepsilon = \varepsilon_{\text{peak}}$  and a variation of interaction time are planed for a further research project.

For microstructure investigations, the compressed samples were cut for both longitudinal (specimen center) and transversal cross sections. The latter sections were chosen at a quarter of the

specimen height. Finite element calculations of the compression tests proved that in this section from the center to half the radius, the local and the global strain rate correspond.

temperature [°C]	pre-strain $2 \times \varepsilon_{\text{peak}}$	strain rate [s <sup>-1</sup> ]				
		0.001	0.01	0.1	1	10
950		0.47	0.59	0.69	0.8	0.91
1050		0.4	0.46	0.55	0.65	0.78
1120		0.35	0.42	0.49	0.58	0.68
1200		0.31	0.36	0.42	0.51	0.61

Table 1: Parameter variation for the experimental investigation of MDRX kinetics.

## Results

**Preparation of the measuring data.** The measurement signals are recorded, depending on the strain rate, with a frequency of 0.1 to 10kHz during deformation. After the deformation stage, the initial frequency of 10kHz is reduced with time: 10kHz for 2s, 3.3kHz for 3s, 1.1kHz for 12s, 0.66kHz for 80s, 0.3kHz for 100s, 0.1kHz for 200s, 0.025kHz for 400s. Because of this scaling the signals of 10 ports are stored within 175000 lines during relaxation. This high density of data is essential to eliminate noise that rely on the induced magnetic field of the conducted specimen. The data filtering has to be done after the test because with band-pass filters of 50Hz, signals reach the data acquisition board with a delay of 20ms. Hence major signal variations directly before and after the deformation stage are stored in a biased manner. The amount of data is reduced after the numerical FFT-process in terms of spline interpolations with equidistant sampling points on the logarithmic time axis. This method implies two advantages: First, the data density is constant in the logarithmic scale. Thus, in non-linear regression calculations all time interceptions are represented by the same weighting. Second, there are no problems in the analysis of different measurement frequencies. This data preparation seems to be very extensive but facilitates the subsequent calculation of the recrystallization kinetics.

**Recrystallization kinetics.** In general, the shape of a stress relaxation curve consists of three stages (see Fig. 3). On the logarithmic scale, linear parts represent stress relaxation due to recovery, whereas a fast decrease of the stress level can be ascribed to SRX or MDRX kinetics. The linear parts can be easily described by tangents (log time equations):

$$\sigma_{\text{appr.}}(t) = \sigma_1 - \alpha_1 \log(t) \quad \text{and} \quad \sigma_{\text{appr.}}(t) = \sigma_2 - \alpha_2 \log(t). \quad (1)$$

The fraction of the recrystallized matrix  $X$  is calculated at first by a rule of mixtures (Eq. 2) [9] and is subsequently fitted via an Avrami approach (Eq. 3) [10]:

$$X_{\text{rx}} = [(\sigma_1 - \alpha_1 \log(t)) - \sigma] / [(\sigma_1 - \sigma_2) - (\alpha_1 - \alpha_2) \log(t)], \quad (2)$$

$$X_{\text{Avrami}} = 1 - [-0.693 \cdot \log(t_{0.5} / t)^n], \quad (3)$$

where  $\sigma_1$ ,  $\alpha_1$ ,  $\sigma_2$  and  $\alpha_2$  are constants,  $\sigma$  is the present stress level,  $t$  is the time,  $t_{0.5}$  is the time for 50% recrystallization and  $n$  is the Avrami exponent. The investigations showed that the slope  $\alpha_1$  always was more negative than  $\alpha_2$ . Thus for high  $X$ , the two tangents converge and the influence of the signal noise on the calculations increase.

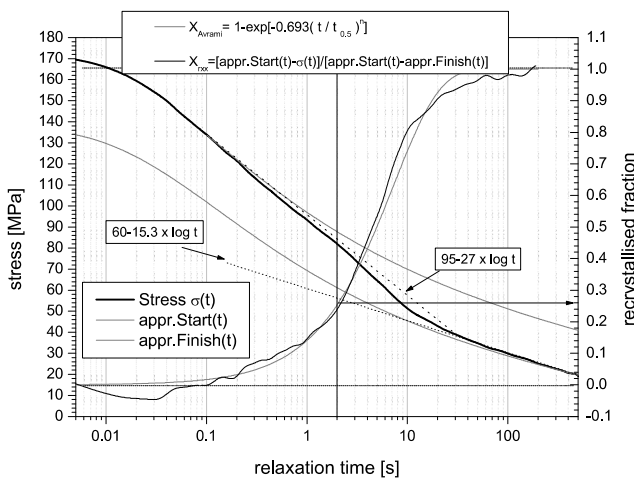


Fig.3: Stress relaxation curve and recrystallized fraction versus time at  $T=1050^{\circ}\text{C}$ ,  $\dot{\epsilon}=0.1\text{s}^{-1}$  and  $\epsilon=0.7\epsilon_{\text{peak}}$ .

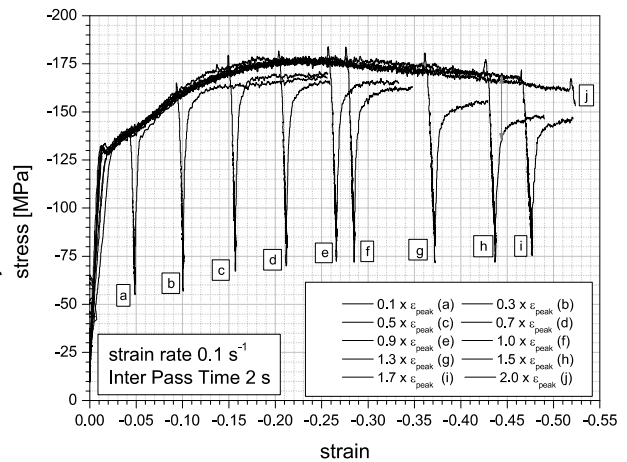


Fig.4: Superposition of stress-strain curves for a series of double hit tests at  $1050^{\circ}\text{C}$ . The curves a-j represent different pre-strains.

Evaluations of the stroke signal indicated that the stroke target could not be reached exactly due to the natural leakage rate of the big valve. Therefore, the servo-hydraulic causes an additional stress release and the compression die moves measurably in the direction of unloading. For this reason, specimens were subject to a very small strain during relaxation.

To validate the applied stress relaxation method, a series of double hit tests with constant pre-strains was carried out. The interval time was set to 2 seconds. Fig. 4 depicts the stress-strain history and shows the increasing softening with increasing pre-strain. If the pre-strains are high enough to produce steady state dynamic recrystallization, saturation of the softening will occur.

A comparison of the double hit test and the stress relaxation method showed that the double hit test leads to slightly higher fractions of recrystallization. A reason for this could be the difference in microstructure in the first and second deformation hit. Fig. 5 and Fig. 6 show the obtained Avrami plots for different pre-strains at a constant strain rate and temperature and for different strain rates at a constant pre-strain and temperature, respectively.

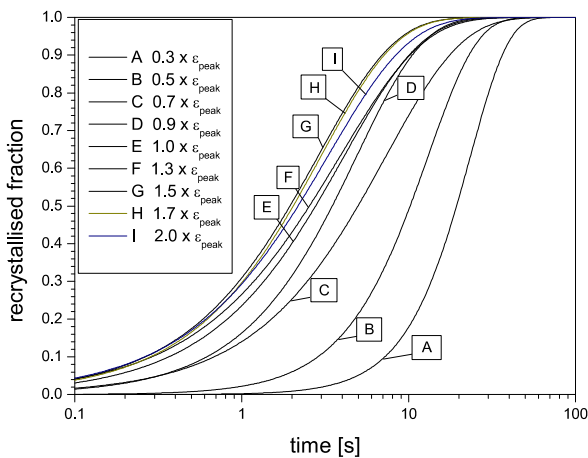


Fig 5: Avrami plots of static and meta-dynamic recrystallization kinetics for  $T=1050^{\circ}\text{C}$  and  $\dot{\epsilon}=0.1\text{s}^{-1}$ .

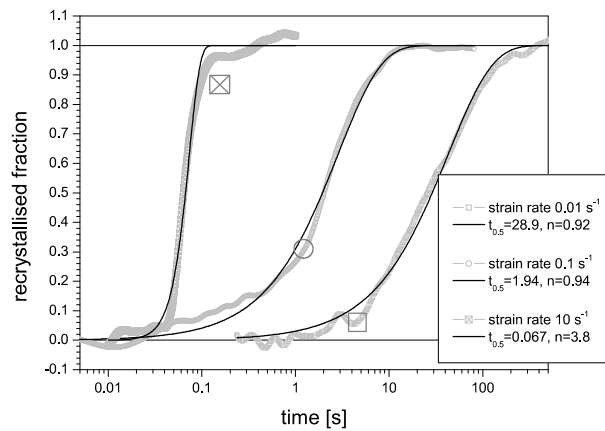


Fig 6: Avrami plots of metadynamic recrystallization kinetics for  $T=1050^{\circ}\text{C}$ ,  $\epsilon=\epsilon_{\text{peak}}$ ,  $\dot{\epsilon}=0.01, 0.1$  and  $10\text{s}^{-1}$ .

## Discussion

The strong influence of the strain rate on MDRX kinetics is of great interest for industrial hot forming processes. Most of the applicable measurement techniques exhibit the problem of a change from isothermal to adiabatic conditions with increasing strain rates. Fig. 2 illustrates an adiabatic case, where recrystallization seems to be finished, before the deformation heat can be dissipated completely and the heating system can react on the changed temperature distribution, respectively. Fig. 6 displays the recrystallization kinetics of the latter case together with smaller strain rates at a temperature target of 1050°C. There is a noticeable increase of the Avrami exponent with strain rate, from ca. 0.9 for small strain rates to 3.8 at  $\dot{\epsilon} = 10 \text{ s}^{-1}$ . This increase can be justified by both additional deformation heat and a higher density of recrystallization nuclei at the same point of time.

Furthermore, the instantaneous heat dissipation after the deformation leads to a negative dilatation and thus probably enforces the stress release. In the case of a strain rate of  $\dot{\epsilon} = 1 \text{ s}^{-1}$  at the same pre-strain as in Fig. 6, recrystallization starts at 0.1s but also the heating system is activated at this moment. Thence a positive thermal sample dilatation initiates an additional compressive stress, which delays the stress release for a short time. Therefore the propagated testing method would point to a retarded recrystallization that could be misinterpreted as the influence of strain induced precipitations, e.g. in HSLA steels.

Further physical and numerical simulation programs will pick these aspects out as a central theme to obtain both a better process reliability and process prediction due to sound physical models and experimental setups.

## References

- [1] G. Wasle: PhD Thesis, Graz University of Technology, Graz, Austria, 2003.
- [2] C. Sommitsch and V. Wieser: EUROMAT 2001 - Proceedings of the 7th European Conference on Advanced Materials and Processes, Rimini, Italy, June 11-14, (2001).
- [3] L. Karjalainen and J. Perttula: ISIJ Int. Vol. 36 (1996), p. 729.
- [4] J. Kömi and L. Karjalainen: Mater. Sci. Tech. Vol. 18 (2002), p. 563.
- [5] R. Djaic and J. Jonas: J. of the Iron and Steel Inst. Vol. 04 (1972), p. 256.
- [6] W.P. Sun and E.B. Hawbolt: ISIJ Int. Vol. 35 (1995), p. 908.
- [7] K.P. Rao, Y.K.D.V. Prasad and E.B. Hawbolt: J. Mater. Proc. Tech. Vol. 77 (1998), p. 166.
- [8] C. Sommitsch, M. Walter, F. Wedl and S. Kleber: Mater. Sci. Forum Vols. 426-432 (2003), p. 743-748.
- [9] L. Karjalainen: Mater. Sci. Tech. Vol. 11 (1995), p. 557.
- [10] C. Sellars: Mater. Sci. Tech. Vol. 6 (1990), p. 1072.

This document is available on the web at <http://www.ttp.net/download>

